

Joint Resummation for Gaugino Pair Production at Hadron Colliders

Jonathan Debove^a, Benjamin Fuks^b, and Michael Klasen^{a,c*}

^a *Laboratoire de Physique Subatomique et de Cosmologie,
Université Joseph Fourier/CNRS-IN2P3/INPG,
53 Avenue des Martyrs, F-38026 Grenoble, France*

^b *Institut Pluridisciplinaire Hubert Curien/Département Recherche Subatomique,
Université de Strasbourg/CNRS-IN2P3,
23 Rue du Loess, F-67037 Strasbourg, France*

^c *Institut für Theoretische Physik, Westfälische Wilhelms-Universität Münster,
Wilhelm-Klemm-Straße 9, D-48149 Münster, Germany*

(Dated: November 6, 2018)

Abstract

We calculate direct gaugino pair production at hadron colliders at next-to-leading order of perturbative QCD, resumming simultaneously large logarithms in the small transverse-momentum and threshold regions to next-to-leading logarithmic accuracy. Numerical predictions are presented for transverse momentum and invariant mass spectra as well as for total cross sections and compared to results obtained at fixed order and with pure transverse-momentum and threshold resummation. We find that our new results are in general in good agreement with the previous ones, but often even more precise.

*klasens@lpsc.in2p3.fr

I. INTRODUCTION

Weak-scale supersymmetry (SUSY), and in particular the Minimal Supersymmetric Standard Model (MSSM), is a theoretically and phenomenologically well-motivated extension of the Standard Model (SM) of particle physics [1]. Consequently, the experimental search for the spin partners predicted by the MSSM for each of the SM particles is one of the defining tasks at current high-energy colliders such as the $p\bar{p}$ Tevatron collider at Fermilab [2] and the pp Large Hadron Collider (LHC) at CERN [3, 4]. Of particular interest are the neutral and charged fermionic partners of the electroweak gauge and Higgs bosons, which mix due to their equal quantum numbers into four neutralino ($\tilde{\chi}_i^0$, $i = 1, \dots, 4$) and chargino ($\tilde{\chi}_i^\pm$, $i = 1, 2$) mass eigenstates, since these participate virtually always in SUSY collider signatures and may also have important implications for dark matter and cosmology. Their decays into leptons and missing transverse energy, carried away by the lightest SUSY particle (LSP, often the $\tilde{\chi}_1^0$), are easily identifiable at hadron colliders. The lighter gaugino/higgsino mass eigenstates are accessible not only at the LHC with center-of-mass energies \sqrt{S} of 7 to 14 TeV [3, 4], but also at Run II of the Tevatron ($\sqrt{S} = 1.96$ TeV), where the production of $\tilde{\chi}_1^\pm \tilde{\chi}_2^0$ pairs decaying into trilepton final states is one of the gold-plated SUSY discovery channels [2].

For an efficient suppression of the SM background from vector-boson and top-quark production and a precise determination of the underlying SUSY-breaking model and masses, an accurate theoretical calculation of the signal (and background) cross section is imperative. As the LSP escapes undetected, the key distribution for SUSY discovery and measurements is the missing transverse-energy (\cancel{E}_T) spectrum, which is typically restricted in the experimental analyses by a cut of 20 GeV at the Tevatron and 30 GeV at the LHC. While the SUSY particle pair is produced with zero transverse momentum (p_T) in the Born approximation, the possible radiation of gluons from the quark-antiquark initial state or the splitting of gluons into quark-antiquark pairs at $\mathcal{O}(\alpha_s)$ in the strong coupling constant induces transverse momenta extending to quite substantial values and must therefore be taken into account. In addition, the perturbative calculation diverges at small p_T , indicating the need for a resummation of soft-gluon radiation to all orders. Only after a consistent matching of the perturbative and resummed calculations an accurate description of the (missing) transverse energy spectrum and precise measurements of the SUSY particle masses can be achieved.

Furthermore, when the SUSY particle pair with invariant mass M is produced close to the production threshold at the partonic center-of-mass energy s , soft gluon emission leads again to potentially large (logarithmic) terms, which must be resummed to all orders in order to obtain a reliable cross section. The production of SUSY particles at hadron colliders has been studied at leading order (LO) of perturbative QCD since the 1980s [5]. More recently, previously neglected electroweak contributions [6], polarization effects [7], and the violation of flavor [8] and CP symmetry [9] have been considered at this order. Next-to-leading order (NLO) corrections have been computed within QCD since the late 1990s [10] and recently also within the electroweak theory [11]. Resummation at the next-to-leading logarithmic (NLL) level has been achieved in the small- p_T region for sleptons and gauginos [12, 13] and in the threshold region for sleptons, gauginos, squarks and gluinos [14, 15].

Since the dynamical origin of the enhanced contributions is the same both in transverse-momentum and threshold resummations, *i.e.* the soft-gluon emission by the initial state, it would be desirable to have a formalism capable to handle at the same time the soft-gluon contributions in both the delicate kinematical regions, $p_T \ll M$ and $M^2 \sim s$. This *joint* resummation formalism has been developed over the last twelve years [16]. The exponentiation of the singular terms in the Mellin (N) and impact-parameter (b) space has been proven, and a consistent method to perform the inverse transforms, avoiding the Landau pole and the singularities of the parton distribution functions (PDFs), has been introduced [17]. Applications to prompt-photon, electroweak and Higgs boson, heavy-quark and slepton pair production at hadron colliders have exhibited substantial effects of joint resummation on the differential and total cross sections [18].

In this paper, we present the first calculation of joint resummation of soft gluon effects in the small transverse momentum and threshold regions for gaugino/higgsino hadroproduction at the NLL level, using the formalism described above. As in our previous calculations [12–15], we include not only the QCD, but also the SUSY-QCD virtual loop contributions with internal squark mixing in the hard coefficient function of the resummed cross section, which therefore reproduces, when expanded and integrated over p_T , the correct NLO SUSY-QCD cross section in the threshold region. For the Tevatron, we consider not only the production of $\tilde{\chi}_1^\pm \tilde{\chi}_2^0$, but also of $\tilde{\chi}_2^0 \tilde{\chi}_2^0$ and $\tilde{\chi}_1^\pm \tilde{\chi}_1^\pm$ pairs. In particular the latter can have significantly larger cross sections than trilepton production due to the s -channel exchange of massless photons. For the LHC, we concentrate on predictions for its current center-of-mass energy

of $\sqrt{S} = 7$ TeV, where threshold effects and direct gaugino pair production (as opposed to the production from squark and gluino cascade decays) will be more important. However, we will also show cross sections for the production of light ($\tilde{\chi}_1^\pm, \tilde{\chi}_2^0$) and heavy ($\tilde{\chi}_2^\pm, \tilde{\chi}_{3,4}^0$) gaugino combinations at the LHC design energy of $\sqrt{S} = 14$ TeV for completeness.

The remainder of this paper is organized as follows: In Sec. II, we briefly review the joint resummation formalism in Mellin and impact parameter space, giving the explicit form of the resummed logarithms at NLL order as well as their matching to the fixed order calculation and the prescriptions employed for the inverse integral transforms. Sec. III contains numerical results for various gaugino pair production cross sections at the Tevatron and at the LHC and compares the results obtained in joint resummation to those obtained with the pure p_T - and threshold resummation formalisms, respectively. We summarize our results in Sec. IV.

II. JOINT RESUMMATION FORMALISM

Thanks to the QCD factorization theorem, the double differential cross section for the hadronic production of a final state with fixed invariant mass M and transverse momentum p_T

$$M^2 \frac{d^2\sigma_{AB}}{dM^2 dp_T^2}(\tau) = \sum_{ab} \int_0^1 dx_a dx_b dz [x_a f_{a/A}(x_a, \mu_F^2)] [x_b f_{b/B}(x_b, \mu_F^2)] [z d\sigma_{ab}(z, M^2, p_T^2, \mu_F^2)] \times \delta(\tau - x_a x_b z) \quad (1)$$

can be obtained by convolving the partonic cross section $d\sigma_{ab}$ with the universal densities $f_{a,b/A,B}$ of the partons a, b , carrying the momentum fractions $x_{a,b}$ of the colliding hadrons A, B , at the factorization scale μ_F . The application of a Mellin transform

$$F(N) = \int_0^1 dy y^{N-1} F(y) \quad (2)$$

to the quantities $F \in \{\sigma_{AB}, \sigma_{ab}, f_{a/A}, f_{b/B}\}$ with $y \in \{\tau = M^2/S, z = M^2/s, x_a, x_b\}$ allows to express the hadronic cross section in moment space as a simple product,

$$M^2 \frac{d^2\sigma_{AB}}{dM^2 dp_T^2}(N-1) = \sum_{ab} f_{a/A}(N, \mu_F^2) f_{b/B}(N, \mu_F^2) \sigma_{ab}(N, M^2, p_T^2, \mu_F^2). \quad (3)$$

Furthermore, the application of a Fourier transform to the partonic cross section σ_{ab} allows to correctly take into account transverse-momentum conservation, so that in moment (N)

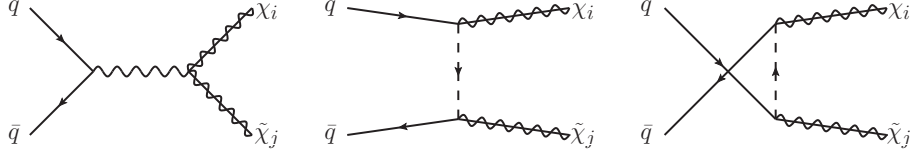


FIG. 1: Tree-level Feynman diagrams for the production of gaugino pairs.

and impact parameter (b) space it can be written as

$$\sigma_{ab}(N, M^2, p_T^2, \mu_F^2) = \int_0^\infty db \frac{b}{2} J_0(bp_T) \sigma_{ab}(N, M^2, b^2, \mu_F^2). \quad (4)$$

Here, $J_0(y)$ denotes the 0th-order Bessel function and

$$\sigma_{ab}(N, M^2, b^2, \mu_F^2) = \sum_{n=0}^{\infty} a_s^n(\mu_R^2) \sigma_{ab}^{(n)}(N, M^2, b^2, \mu_F^2, \mu_R^2) \quad (5)$$

is usually expanded perturbatively in the strong coupling constant $a_s(\mu^2) = \alpha_s(\mu^2)/(2\pi)$ at the renormalization scale μ_R . For simplicity, we identify in the following the factorization and renormalization scales, *i.e.* $\mu_F = \mu_R = \mu$.

In the Born approximation, the hadroproduction of neutralinos $\tilde{\chi}_i^0$ and charginos $\tilde{\chi}_i^\pm$ is induced by quarks q and antiquarks \bar{q}' in the initial (anti-)protons and is mediated by s -channel electroweak gauge-boson and t - and u -channel squark exchanges (see Fig. 1). Its partonic cross section $\sigma_{q\bar{q}'}^{(0)}$ can be expressed in terms of the gaugino and squark masses $m_{\tilde{\chi}_{i,j}^{0,\pm}}$ and $m_{\tilde{q}}$, the masses of the electroweak gauge bosons, and generalized charges [5]. At $\mathcal{O}(a_s)$, virtual loop and real parton emission corrections must be taken into account [10]. The latter induce not only a deviation of the partonic center-of-mass energy s from the squared invariant mass M^2 of the gaugino pair, but also non-zero transverse momenta p_T , that extend typically to values of the order of the gaugino mass.

Close to the partonic production threshold, where $z = M^2/s \rightarrow 1$ or $N \rightarrow \infty$, the convergence of the perturbative expansion is spoiled due to soft gluon radiation, which induces large logarithms

$$a_s^n \left(\frac{\ln^m(1-z)}{1-z} \right)_+ \rightarrow a_s^n \ln^{m+1} \bar{N} + \dots \quad (6)$$

with $m \leq 2n - 1$ and $\bar{N} = Ne^{\gamma_E}$ [15]. Similarly, in the small- p_T (or large- b) region, where the bulk of the events is produced, the convergence of the perturbative expansion is again spoiled by soft gluon radiation, which induces large logarithms

$$\alpha_s^n \left(\frac{1}{p_T^2} \ln^m \frac{M^2}{p_T^2} \right)_+ \rightarrow \alpha_s^n \ln^{m+1} \bar{b}^2 + \dots \quad (7)$$

with $m \leq 2n - 1$ and $\bar{b} = bMe^{\gamma_E}/2$ [13]. The crucial observation, first made by Li [16] and then further developed by Laenen, Sterman, and Vogelsang [17, 18] is that the common kinematic origin of these divergences allows for a joint resummation of the large logarithms in the partonic cross section by choosing a function

$$\chi(\bar{N}, \bar{b}) = \frac{\bar{N}}{1 + \eta \bar{b}/\bar{N}} + \bar{b}, \quad (8)$$

which interpolates between \bar{N} in the threshold region, $\bar{N} \gg \bar{b}$, and \bar{b} in the small- p_T region, $\bar{b} \gg \bar{N}$. Its exact form is constrained by the requirement that the leading and next-to-leading logarithms in \bar{b} and \bar{N} are correctly reproduced in the limits $\bar{b} \rightarrow \infty$ and $\bar{N} \rightarrow \infty$, respectively. The choice of Eq. (8) with $\eta > 0$ (we use $\eta = 1$) avoids the introduction of sizeable subleading terms into perturbative expansions of the resummed cross section at a given order in a_s , which are not present in fixed-order calculations [18]. Up to NLL order, the resummed cross section can then be written in the form

$$\begin{aligned} \sigma_{ab}(N, M^2, b^2, \mu^2) &= \sum_{a', a'', b', b''} E_{a'a}^{(1)}(N, M^2/\chi^2, \mu^2) E_{b'b}^{(1)}(N, M^2/\chi^2, \mu^2) C_{a''a'}(N, a_s(M^2/\chi^2)) \\ &\times C_{b''b'}(N, a_s(M^2/\chi^2)) H_{a''b''}(M^2, \mu^2) \exp[G_{a''b''}(M^2, \bar{N}, \bar{b}^2, \mu^2)], \end{aligned} \quad (9)$$

which is very similar to the one of the p_T -resummed cross section. The operators $E_{a'a, b'b}$ allow to evolve the PDFs $f_{a, b/A, B}(N, \mu^2)$ from the scale μ^2 to the scale M^2/χ^2 . They satisfy, like the PDFs themselves, the Altarelli-Parisi equations [19] and can be written to one-loop order, $E^{(1)}$, and in the singlet/non-singlet basis in closed exponential form [20]. When the finite part of the renormalized virtual one-loop contribution \mathcal{A}_0 , which in our calculation contains the full SUSY-QCD corrections with internal squark mixing [15], is entirely absorbed into the hard function

$$H_{ab}(M^2, \mu^2) = \sigma_{ab}^{(0)}(M^2, \mu^2) [1 + a_s \mathcal{A}_0] + \mathcal{O}(a_s^2), \quad (10)$$

the coefficients C_{ab} become process-independent and can be written up to one-loop order as $C_{ab}^{(0)} = \delta_{ab}$ and

$$C_{ab}^{(1)}(N) = C_a \frac{\pi^2}{6} \delta_{ab} - P_{ab}^{(1), \epsilon}(N), \quad (11)$$

where $C_{ab} = \sum_{n=0}^{\infty} a_s^n(\mu_R^2) C_{ab}^{(n)}$, the QCD color factors are $C_q = C_F = 4/3$ and $C_g = C_A = 3$,

respectively, and

$$P_{qq}^{(1),\epsilon}(N) = \frac{-C_F}{N(N+1)} \quad , \quad P_{qg}^{(1),\epsilon}(N) = \frac{-2T_R}{(N+1)(N+2)}, \quad (12)$$

$$P_{gq}^{(1),\epsilon}(N) = \frac{-C_F}{N+1} \quad , \quad P_{gg}^{(1),\epsilon}(N) = 0 \quad (13)$$

represent the $\mathcal{O}(a_s, \epsilon)$ terms in the Altarelli-Parisi splitting functions in Mellin space with $T_R = 1/2$. The important feature of Eq. (9) is that the hard function $H_{ab}(M^2, \mu^2)$, contrary to the perturbative cross section $\sigma_{ab}(N, M^2, b^2, \mu^2)$ in Eq. (5), no longer contains large logarithms in either \bar{N} or \bar{b} , since these have all been resummed in the coefficient functions C , the evolution operators E , and the Sudakov exponent G . The latter can be expanded as

$$G_{ab}(M^2, \bar{N}, \bar{b}^2, \mu^2) = Lg_{ab}^{(1)}(\lambda) + g_{ab}^{(2)}(\lambda, \ln \bar{N}, M^2/\mu^2) + \dots \quad (14)$$

where $L = \ln \chi = \lambda/(a_s \beta_0)$ encodes the large logarithms in both \bar{N} and \bar{b} , $\beta_0 = 11C_A/6 - 2N_f T_R/3$ is the one-loop coefficient of the QCD beta-function, and N_f is the number of active quark flavors. The first term in this expansion

$$Lg_{ab}^{(1)}(\lambda) = \frac{L}{2\lambda\beta_0}(A_a^{(1)} + A_b^{(1)})[2\lambda + \ln(1 - 2\lambda)] \quad (15)$$

collects the leading logarithmic (LL) contributions, while the second term

$$\begin{aligned} 2\beta_0 g_{ab}^{(2)}(\lambda, \ln \bar{N}, M^2/\mu^2) &= (A_a^{(1)} + A_b^{(1)}) \left[2\lambda \frac{1 - 2a_s \beta_0 \ln \bar{N}}{1 - 2\lambda} + \ln(1 - 2\lambda) \right] \ln \frac{M^2}{\mu^2} \\ &+ (A_a^{(1)} + A_b^{(1)}) \frac{\beta_1}{\beta_0^2} \left[(2\lambda + \ln(1 - 2\lambda)) \frac{1 - 2a_s \beta_0 \ln \bar{N}}{1 - 2\lambda} + \frac{1}{2} \ln^2(1 - 2\lambda) \right] \\ &- (A_a^{(2)} + A_b^{(2)}) \frac{1}{\beta_0} \left[2\lambda \frac{1 - 2a_s \beta_0 \ln \bar{N}}{1 - 2\lambda} + \ln(1 - 2\lambda) \right] \\ &+ (-2\gamma_a^{(1)} - 2\gamma_b^{(1)} + D_{ab}^{(1)}) \ln(1 - 2\lambda) \end{aligned} \quad (16)$$

with $\beta_1 = (17C_A^2 - 5C_A N_f - 3C_F N_f)/6$ collects the NLL contributions. These terms reproduce those appearing in the transverse-momentum resummation formalism [13], when $\bar{b} \gg \bar{N}$, $\chi \rightarrow \bar{b}$ and $(1 - 2a_s \beta_0 \ln \bar{N})/(1 - 2\lambda) \rightarrow 1/(1 - 2\lambda)$, as well as those appearing in the threshold resummation formalism [15], when $\bar{N} \gg \bar{b}$, $\chi \rightarrow \bar{N}$ and $(1 - 2a_s \beta_0 \ln \bar{N})/(1 - 2\lambda) \rightarrow 1$, respectively. For transverse-momentum resummation, the logarithm ($\ln \bar{b}$) had to be modified (to $\ln \sqrt{1 + \bar{b}^2}$) in order to suppress unphysical resummation contributions at large p_T and small \bar{b} . This is not necessary within the joint resummation formalism, as the small- \bar{b} singularity is regularized through the function $\chi(\bar{N}, \bar{b})$. The coefficients

$$A_a^{(1)} = 2C_a \quad , \quad A_a^{(2)} = 2C_a \left[\left(\frac{67}{18} - \frac{\pi^2}{6} \right) C_A - \frac{5}{9} N_f \right] \quad \text{and} \quad D_{ab}^{(1)} = 0 \quad (17)$$

are well-known from both threshold and transverse-momentum resummation [21], while the anomalous dimensions

$$\gamma_q^{(1)} = \frac{3C_F}{2}, \quad \gamma_g^{(1)} = \beta_0 \quad (18)$$

of the quark and gluon fields have been introduced in order to remove the corresponding NLL terms from the one-loop approximation of the diagonal evolution operators $E_{aa}^{(1)}$.

While the large logarithms must clearly be resummed close to the production threshold, when $z \rightarrow 1$ and $\bar{N} \rightarrow \infty$, and/or at small values of $p_T \rightarrow 0$, when $\bar{b} \rightarrow \infty$, they account only partially for the full perturbative cross section away from these regions. In order to obtain a valid cross section at all values of z and p_T , the fixed-order (f.o.) and the resummed (res.) calculations must be combined consistently by subtracting from their sum the perturbatively expanded (exp.) resummed component,

$$\sigma_{ab} = \sigma_{ab}^{(\text{res.})} + \sigma_{ab}^{(\text{f.o.})} - \sigma_{ab}^{(\text{exp.})}. \quad (19)$$

The latter is easily obtained by expanding Eq. (4) to the desired accuracy. At $\mathcal{O}(a_s)$, one finds

$$\begin{aligned} \sigma_{ab}^{(\text{exp.})}(N, M^2, p_T^2, \mu^2) &= H_{ab}^{(0)}(M^2, \mu^2) + a_s H_{ab}^{(1)}(M^2, \mu^2) \\ &- a_s \left(2\mathcal{J} - \ln \frac{M^2}{\mu^2} \right) \sum_c [H_{ac}^{(0)}(M^2, \mu^2) P_{cb}^{(1)}(N) + P_{ca}^{(1)}(N) H_{cb}^{(0)}(M^2, \mu^2)] \\ &+ a_s \sum_c [H_{ac}^{(0)}(M^2, \mu^2) C_{cb}^{(1)}(N) + C_{ca}^{(1)}(N) H_{cb}^{(0)}(M^2, \mu^2)] \\ &- a_s H_{ab}^{(0)}(M^2, \mu^2) [\mathcal{J}^2 (A_a^{(1)} + A_b^{(1)}) - 2\mathcal{J}(\gamma_a^{(1)} + \gamma_b^{(1)})], \end{aligned} \quad (20)$$

where the $\mathcal{O}(a_s, \epsilon^0)$ terms of the Altarelli-Parisi splitting functions are

$$P_{qq}^{(1)}(N) = C_F \left[\frac{3}{2} + \frac{1}{N(N+1)} - 2 \sum_{k=1}^N \frac{1}{k} \right], \quad (21)$$

$$P_{gq}^{(1)}(N) = C_F \left[\frac{2 + N + N^2}{N(N^2 - 1)} \right], \quad (22)$$

$$P_{qg}^{(1)}(N) = T_R \left[\frac{2 + N + N^2}{N(N+1)(N+2)} \right], \quad (23)$$

$$P_{gg}^{(1)}(N) = 2C_A \left[\frac{1}{N(N-1)} + \frac{1}{(N+1)(N+2)} - \sum_{k=1}^N \frac{1}{k} \right] + \beta_0, \quad (24)$$

and the full dependence on the transverse momentum p_T is embodied in the Bessel integral

$$\mathcal{J} = \int_0^\infty db \frac{b}{2} J_0(bp_T) \ln \chi(\bar{N}, \bar{b}). \quad (25)$$

The form of this integral has been chosen to match the one encountered in p_T -resummation. Unfortunately, it then induces π^2 -terms which differ slightly from those encountered in threshold resummation [18]. While these terms are formally beyond NLL order, one should nevertheless expect slightly better numerical agreement with the p_T -resummed calculation than with the threshold-resummed calculation.

After the resummation of the partonic cross section has been performed in N - and b -space, we have to multiply the resummed cross section and its perturbative expansion with the moments of the PDFs $f_{a/A}(N, \mu^2)$ and transform the hadronic cross section obtained in this way back to the physical z - and p_T -spaces. The moments of the PDFs are obtained through a numerical fit to the publicly available PDF parameterizations in x -space. For the inverse integral transforms, special attention has to be paid to the singularities in the resummed exponents, *i.e.* when $\lambda = 1/2$ in Eqs. (15) and (16). They are related to the presence of the Landau pole in the perturbative running of $a_s(\mu^2)$, and prescriptions for both the Mellin and Fourier inverse transforms are needed. For the Fourier inverse transform of Eq. (4), we follow Ref. [17] and deform the integration contour of the b -integral in the complex plane by defining two integration branches

$$b = (\cos \varphi \pm i \sin \varphi)t, \quad t \in [0, \infty[, \quad (26)$$

where φ has to be chosen in the range $]0, \pi/2[$. The Bessel function $J_0(y)$ in Eq. (4) is then replaced by the sum of the two auxiliary functions

$$h_1(y, v) = -\frac{1}{2\pi} \int_{-iv\pi}^{-\pi+iv\pi} d\theta e^{-iy \sin \theta}, \quad (27)$$

$$h_2(y, v) = -\frac{1}{2\pi} \int_{\pi+iv\pi}^{-iv\pi} d\theta e^{-iy \sin \theta}, \quad (28)$$

which are finite for any value of y . Their sum is independent of v and is always equal to $J_0(y)$. Since the two functions distinguish positive and negative phases in the complex b -plane, they can be associated with only one of the two branches. For the inverse Mellin transform

$$F(y) = \int_{\mathcal{C}_N} \frac{dN}{2\pi i} y^{-N} F(N) \quad (29)$$

we choose an integration contour \mathcal{C}_N according to the principal value procedure proposed in Ref. [22] and the minimal prescription proposed in Ref. [23] and define again two branches

$$\mathcal{C}_N : \quad N = C + ye^{\pm i\phi}, \quad y \in [0, \infty[. \quad (30)$$

The parameter C must be chosen in such a way that the poles in the Mellin moments of the parton densities, which are related to the small- x (Regge) singularity $f_{a/A}(x, \mu_0^2) \propto x^\alpha(1-x)^\beta$ with $\alpha < 0$, lie to the left and the Landau pole to the right of the integration contour, respectively. While formally the angle ϕ can be chosen in the range $[\pi/2, \pi[$, it is advantageous to take $\phi > \pi/2$ to improve the convergence of the inverse Mellin transform.

III. NUMERICAL RESULTS

We now turn to our numerical analysis of joint resummation effects on the production of various gaugino pairs at the Tevatron $p\bar{p}$ -collider ($\sqrt{S} = 1.96$ TeV) and the LHC pp -collider ($\sqrt{S} = 7 - 14$ TeV). For the masses and widths of the electroweak gauge bosons, we use the values of $m_Z = 91.1876$ GeV and $m_W = 80.403$ GeV [24]. The CKM-matrix is assumed to be diagonal, and the top quark mass is taken to be 173.1 GeV [25]. The strong coupling constant is evaluated in the one-loop and two-loop approximation for LO and NLO/NLL+NLO results, respectively, with a value of $\Lambda_{\overline{\text{MS}}}^{n_f=5}$ corresponding to the employed LO (CTEQ6L1) and NLO (CTEQ6.6M) parton densities [26]. For the resummed and expanded contributions, the latter have been transformed numerically to Mellin N -space. When we present spectra in the invariant mass M of the gaugino pair, we identify the unphysical scales $\mu_F = \mu_R = \mu$ with M , whereas for transverse momentum distributions and total cross sections we identify them with the average mass of the two produced gauginos. The remaining theoretical uncertainty is estimated by varying the common scale μ about these central values by a factor of two up and down. The running electroweak couplings as well as the physical masses of the SUSY particles and their mixing angles are computed with the computer program SPheno 2.2.3 [27], which includes a consistent calculation of the Higgs boson masses and all one-loop and the dominant two-loop radiative corrections in the renormalization group equations linking the restricted set of SUSY-breaking parameters at the gauge coupling unification scale to the complete set of observable SUSY masses and mixing angles at the electroweak scale.

For the Tevatron, we choose the low-mass point LM0 (SU4) with universal fermion mass $m_{1/2} = 160$ GeV, scalar mass $m_0 = 200$ GeV, trilinear coupling $A_0 = -400$ GeV, bilinear Higgs mass parameter $\mu > 0$, and ratio of Higgs vacuum expectation values $\tan\beta = 10$ [3, 28]. It has been defined by the CMS (ATLAS) collaboration with the objective of

high cross sections and thus early discovery at the LHC, as the resulting gaugino, squark and slepton masses $m_{\tilde{\chi}_2^0} = m_{\tilde{\chi}_1^\pm} = 113$ GeV, $m_{\tilde{\chi}_1^0} = 61$ GeV, $m_{\tilde{q}} \simeq 420$ GeV, and $m_{\tilde{l}} \simeq 220$ GeV lie just beyond the current Tevatron limits. In this scenario, the lightest chargino and second-lightest neutralino decay with 35% and 15% probability through virtual sleptons to the LSP and one and two charged leptons, respectively [29].

For the LHC, we choose the widely used minimal supergravity (mSUGRA) point SPS1a' [30] as the benchmark for our numerical studies. This point has the same intermediate value of $\tan\beta = 10$ and $\mu > 0$ (favored by the rare decay $b \rightarrow s\gamma$ and the measured anomalous magnetic moment of the muon), a still relatively small gaugino mass parameter of $m_{1/2} = 250$ GeV, and a slightly lower scalar mass parameter $m_0 = 70$ GeV and trilinear coupling $A_0 = -300$ GeV than the original point SPS1a [31] in order to render it compatible with low-energy precision data, high-energy mass bounds, and the observed cold dark matter relic density. It is also similar to the post-WMAP point B' ($m_0 = 60$ GeV and $A_0 = 0$) [32], which has been adopted by the CMS collaboration as their low-mass point LM1 [4]. In the SPS1a' scenario, the $\tilde{\chi}_1^0$ is the LSP with a mass of 98 GeV, the gauginos producing the trilepton signal have masses of $m_{\tilde{\chi}_1^\pm} \simeq m_{\tilde{\chi}_2^0} = 184$ GeV, and the heavier gauginos, which decay mostly into the lighter gauginos, W and Z bosons as well as the lightest Higgs boson, have masses of $m_{\tilde{\chi}_3^0} = 400$ GeV and $m_{\tilde{\chi}_2^\pm} \simeq m_{\tilde{\chi}_4^0} = 415$ GeV. The average squark and gluino masses are $m_{\tilde{q}} \simeq 550$ GeV and $m_{\tilde{g}} = 604$ GeV. Note that this benchmark point is also relatively close to the region excluded by the Tevatron collaborations CDF and D0, which assume, however, a lower value of $\tan\beta = 3$ and $A_0 = 0$ [2].

A. Transverse momentum spectra

In Fig. 2, we present transverse momentum spectra for light charged and neutral gaugino pairs with masses of 113 and 184 GeV at the Tevatron (top) and early LHC (bottom), where the center-of-mass energies are $\sqrt{S} = 1.96$ and 7 TeV, respectively. We show predictions at fixed order $\mathcal{O}(\alpha_s)$ (dashed) as well as with transverse-momentum (dotted) and joint resummation (full curves). While the fixed-order predictions diverge at small p_T due to an uncanceled soft singularity from real gluon emission, the resummed predictions exhibit a finite, physical behavior with a pronounced maximum in the region of $p_T = 5$ to 10 GeV. In the region of intermediate p_T of 20 to 60 GeV, the resummed predictions are considerably

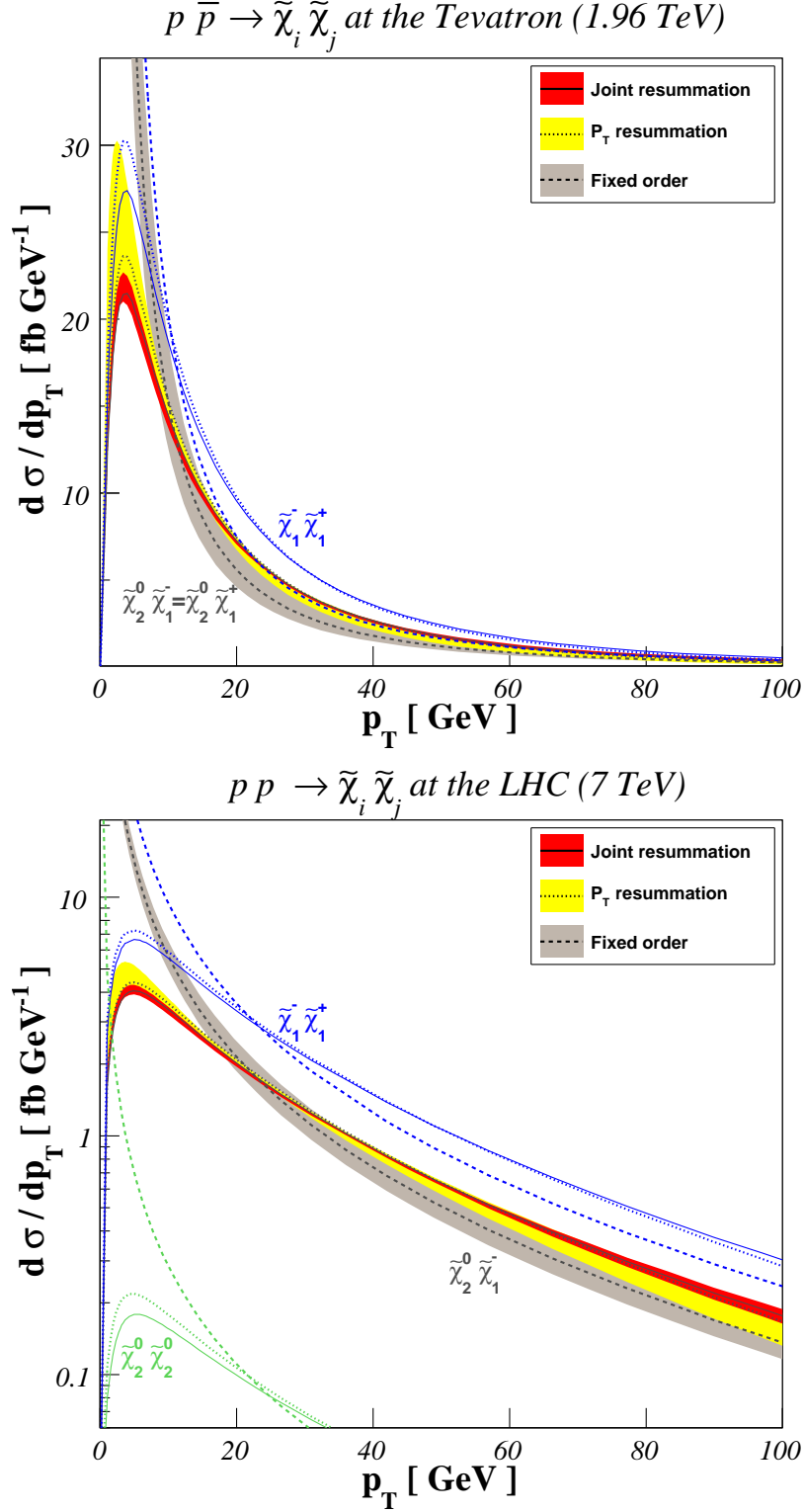


FIG. 2: Transverse momentum distributions of light gaugino pairs at the Tevatron (top) and LHC (bottom) with $\sqrt{S} = 1.96$ and 7 TeV center-of-mass energy, respectively, in fixed order (dashed) as well as with transverse-momentum (dotted) and joint (full curves) resummation.

larger than those at fixed order. The calculations using transverse-momentum and joint resummation are in good agreement, but the theoretical uncertainty of the latter, estimated by varying the renormalization and factorization scales by a factor of two about the average mass of the two gauginos, is considerably smaller, since threshold logarithms are resummed simultaneously. The cross sections for chargino pairs exceed those for the trilepton channel at the Tevatron and for the $\tilde{\chi}_2^0\tilde{\chi}_1^-$ channel (but not the $\tilde{\chi}_2^0\tilde{\chi}_1^+$ channel, which is not shown) at the early LHC with the cross section for pair production of the second-lightest neutralino being more than an order of magnitude smaller at the early LHC.

At the LHC design luminosity of $\sqrt{S} = 14$ TeV, the neutralino pair production cross section is larger by more than a factor of three (see the top part of Fig. 3). Otherwise, the behavior of the various predictions is very similar to the one described above. One notices, however, that the resummed predictions exceed those at fixed order only at larger values of $p_T > 40$ GeV. Furthermore, the trilepton cross section for positive charginos is larger than the one for negative charginos by almost a factor of two, since in contrast to the Tevatron the LHC is a pp collider. With a center-of-mass energy of $\sqrt{S} = 14$ TeV, it may also become possible to observe the associated production of heavier neutralinos $\tilde{\chi}_4^0$ and charginos $\tilde{\chi}_2^\pm$ with masses of about 415 GeV. The corresponding transverse momentum spectra are shown in the lower part of Fig. 3. The absolute values of the cross sections are reduced by about a factor of 50 for both positive and negative charginos, but the shape of the distributions is very similar. Joint resummation leads again to the smallest scale uncertainties.

B. Invariant mass spectra

While the joint resummation formalism is designed to match more closely the one for transverse-momentum resummation, it also allows to simultaneously resum threshold logarithms and obtain precise invariant mass spectra. These are therefore presented in this section for various gaugino pairs and colliders and compared to those obtained with pure threshold resummation with the expectation that the agreement will be slightly worse than the one for transverse momentum distributions.

In Fig. 4 we show invariant mass spectra for the trilepton channel at the Tevatron obtained at LO (short-dashed) and with NLO SUSY-QCD corrections (dashed) as well as with pure threshold (dotted) and joint (full curve) resummation. In this figure, the NLO and threshold

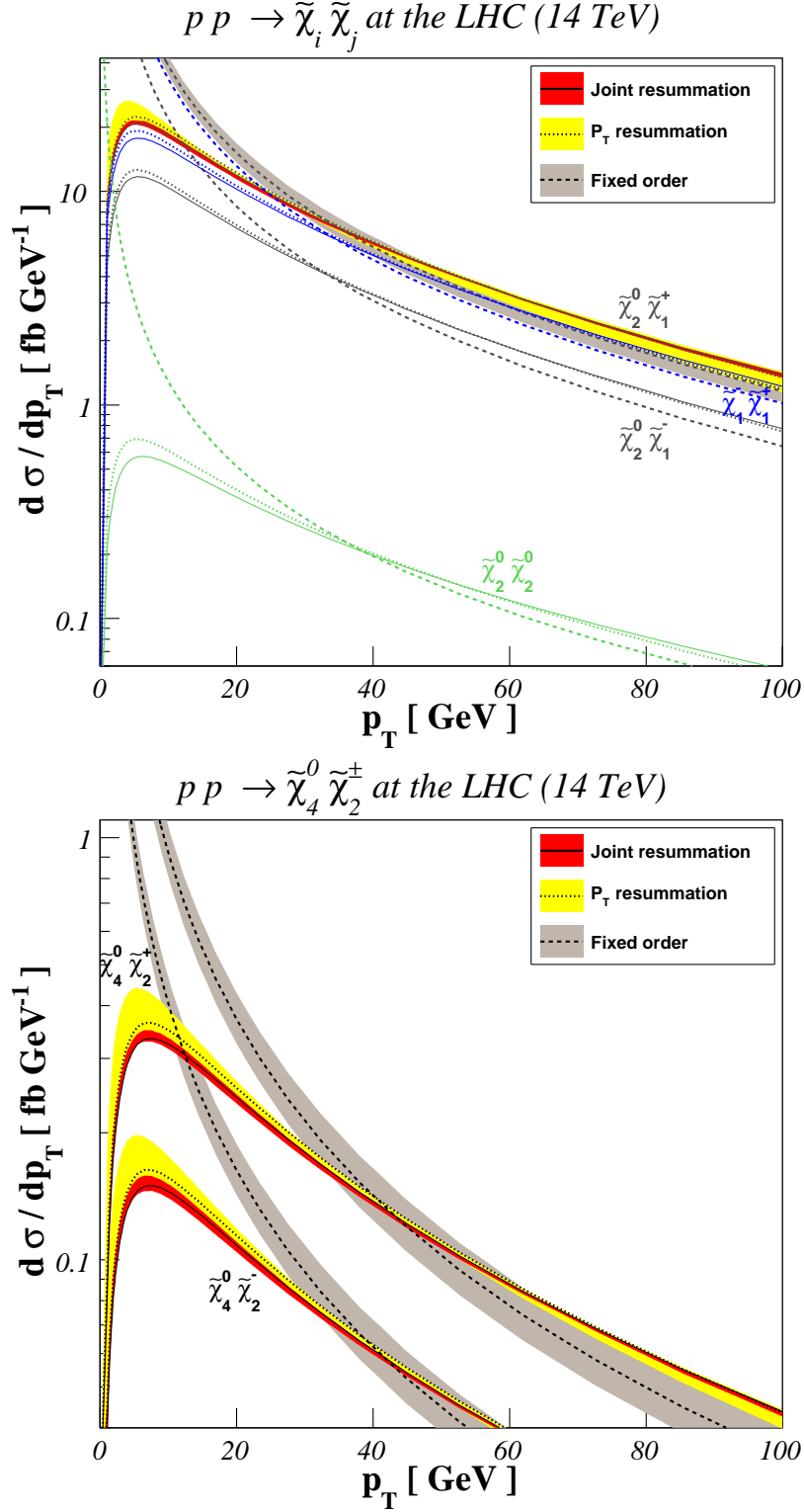


FIG. 3: Transverse momentum distributions of light (top) and heavy (bottom) gaugino pairs at the LHC with $\sqrt{S} = 14$ TeV center-of-mass energy in fixed order (dashed) as well as with transverse-momentum (dotted) and joint (full curves) resummation.

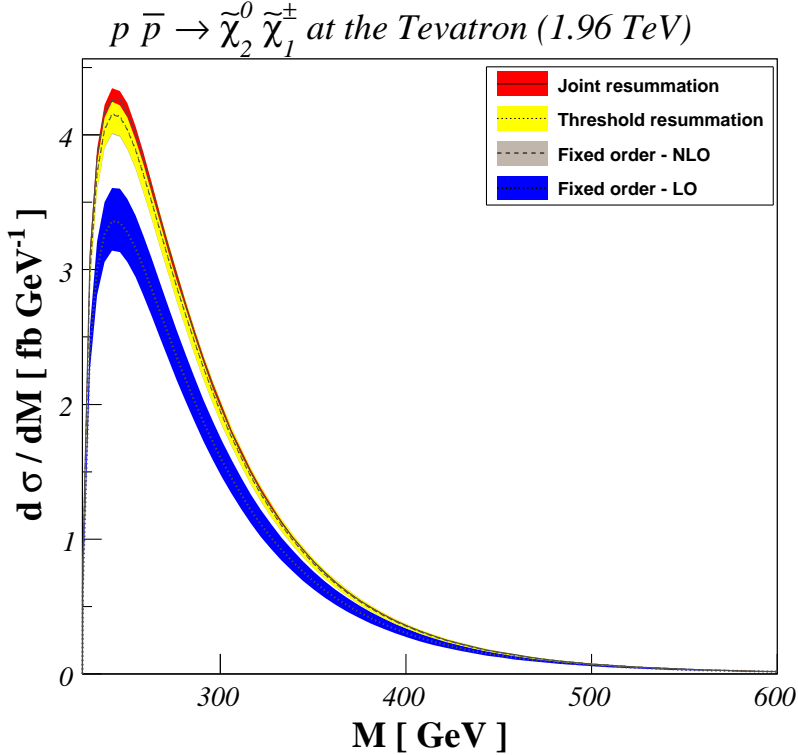


FIG. 4: Invariant mass distributions of light gaugino pairs at the Tevatron with $\sqrt{S} = 1.96$ TeV center-of-mass energy in fixed order (short-dashed, dashed) as well as with threshold (dotted) and joint (full curve) resummation.

resummed predictions are both considerably larger than the one obtained at LO. In the linear representation of $d\sigma/dM$ emphasizing the low-invariant mass region shown here, they can in fact not be distinguished, as threshold effects only start to dominate as the invariant mass squared M^2 approaches the total available center-of-mass energy \sqrt{s} . This is also the reason why the jointly resummed prediction differs and in fact exceeds slightly the pure threshold resummed prediction at small M , as large logarithms at small p_T have been simultaneously resummed. This leads also to an additional reduction of the scale uncertainty, represented again as a shaded band and obtained by varying the renormalization and factorization scales by a factor of two about the invariant mass M .

The various features described above are even more prominent at the LHC with its larger design center-of-mass energy of $\sqrt{S} = 14$ TeV, despite the fact that also the masses of the light gauginos are slightly larger in the SPS1a' scenario than at the LM0 benchmark point. The scale uncertainties in the upper part of Fig. 5 are considerably smaller at LO and even

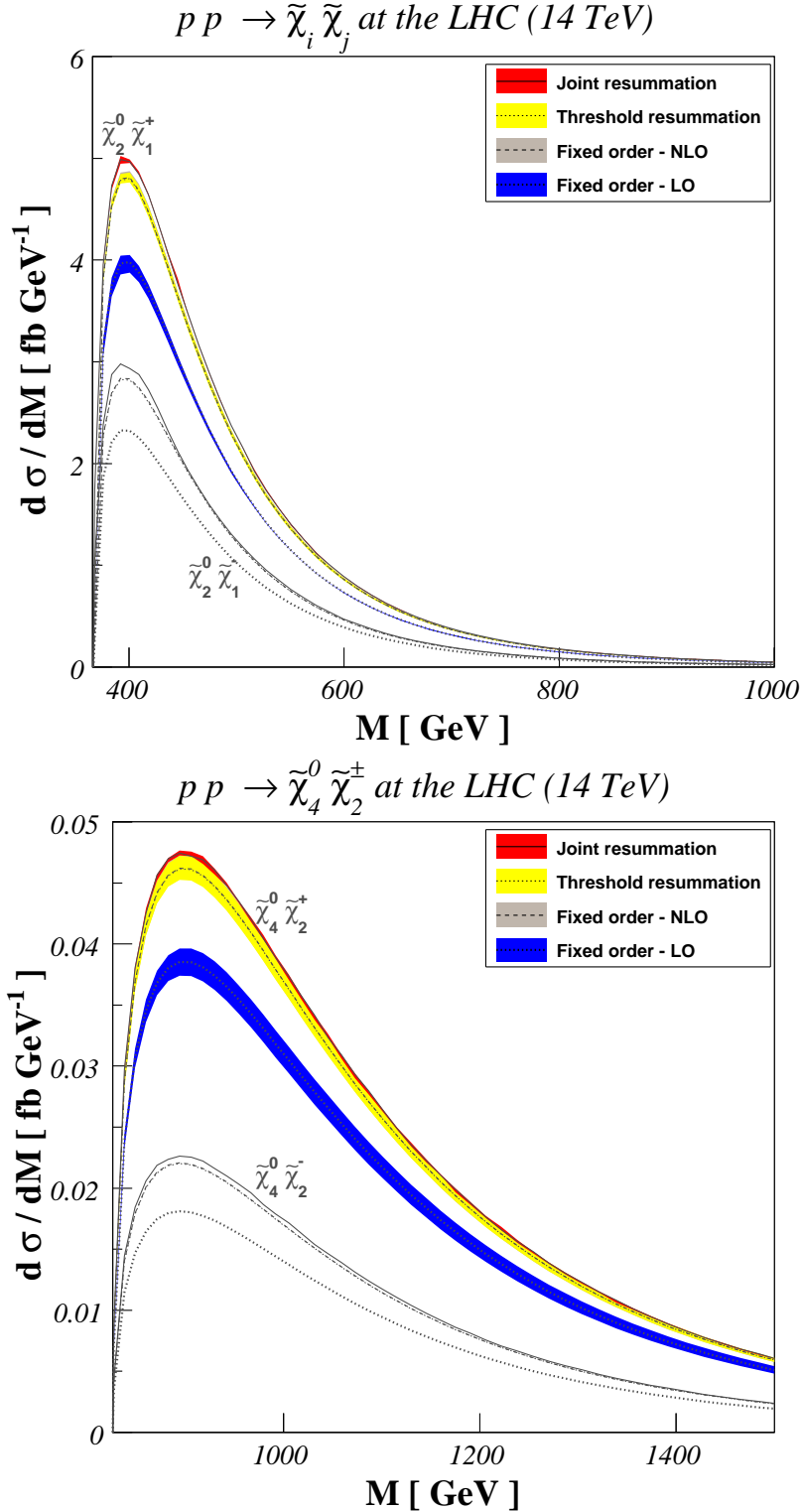


FIG. 5: Invariant mass distributions of light (top) and heavy (bottom) gaugino pairs at the LHC with $\sqrt{S} = 14$ TeV center-of-mass energy in fixed order (short-dashed, dashed) as well as with threshold (dotted) and joint (full) resummation.

more at NLO and NLL+NLO, as the variation from $M/2$ to $2M$ is less important compared to the large \sqrt{S} . This leads to threshold and joint resummation predictions that no longer overlap within scale uncertainties in the region of maximal cross section, indicating that the theoretical error is slightly underestimated in this case. As it was already observed in the previous section, the cross section for the trilepton channel with positive charge exceeds the negative one by almost a factor of two due to the positively charged initial state at the LHC. Heavier gauginos are produced closer to threshold, so that the distributions in the lower part of Fig. 5 are found at larger values of M . The scale variation and the shaded bands representing it become more important again with respect to \sqrt{S} as do the threshold logarithms, so that the threshold and jointly resummed predictions overlap again within the theoretical uncertainties. The absolute size of the cross section is again almost two times larger for $\tilde{\chi}_4^0\tilde{\chi}_2^+$ pairs than for $\tilde{\chi}_4^0\tilde{\chi}_2^-$ pairs.

C. Total cross sections

Total cross sections can be obtained from the distributions shown in the previous sections by integrating over either p_T or M . This is numerically not always trivial, but should in principle lead to similar predictions, building confidence in the theoretical calculations. In particular, since the perturbative, resummed and expanded contributions are obtained in (p_T, M) and (b, N) space, respectively, we first compute the differential cross section $d\sigma/dp_T$ and then integrate over p_T with the trapezoidal rule only after the different contributions to the total cross section have been matched.

The results are displayed in Tab. I. They show the expected important increase in absolute size and reduction in scale uncertainty from LO to NLO and then, to a lesser extent, at NLL+NLO. It is interesting to note that the p_T -resummed predictions are indeed larger than those obtained at NLO, but the threshold resummed predictions are slightly smaller. The jointly resummed predictions are very similar to those obtained at NLO at the two lower center-of-mass energies and larger at the LHC with $\sqrt{S} = 14$ TeV. As expected, the lowest scale uncertainties are found with threshold resummation when the particle masses are large compared to the available center-of-mass energy (light gauginos at the Tevatron, heavy gauginos at the LHC with $\sqrt{S} = 14$ TeV), while joint resummation gives results that are similar to p_T resummation, but more precise, in the two other cases.

TABLE I: Total cross sections (in fb) with scale uncertainties for the trilepton channel at the Tevatron in the LM0 scenario and for light and heavy gaugino pairs at the LHC with 7 and 14 TeV center-of-mass energy in the SPS 1a' scenario at various levels of accuracy.

Collider	Gauginos	LO	NLO	p_T	Threshold	Joint
Tevatron	$\tilde{\chi}_2^0 \tilde{\chi}_1^\pm$	$300.044^{+27.555}_{-23.707}$	$366.794^{+10.772}_{-11.750}$	$377.118^{+5.891}_{-14.548}$	$363.922^{+1.702}_{-2.801}$	$365.974^{+3.542}_{-3.847}$
LHC-7	$\tilde{\chi}_2^0 \tilde{\chi}_1^-$	$102.245^{+3.494}_{-3.564}$	$121.216^{+1.843}_{-1.557}$	$122.817^{+1.338}_{-1.302}$	$119.885^{+0.118}_{-0.632}$	$121.188^{+0.084}_{-0.590}$
LHC-14	$\tilde{\chi}_2^0 \tilde{\chi}_1^-$	$346.538^{+2.210}_{-4.862}$	$419.930^{+4.016}_{-1.809}$	$429.678^{+0.962}_{-1.605}$	$416.327^{+0.895}_{-2.547}$	$428.202^{+0.464}_{-2.680}$
LHC-14	$\tilde{\chi}_4^0 \tilde{\chi}_2^-$	$6.506^{+0.308}_{-0.291}$	$7.844^{+0.140}_{-0.133}$	$8.261^{+0.179}_{-0.174}$	$7.763^{+0.017}_{-0.008}$	$8.117^{+0.033}_{-0.047}$

IV. CONCLUSION

In this paper, we have completed our investigation of gaugino production at hadron colliders with different resummation methods by presenting a NLL+NLO calculation that jointly resums large logarithms in the small- p_T and threshold regions. After a detailed outline of the organization of the analytical calculation and the numerical implementation, in particular of the convolutions with the parton densities and the inverse Fourier and Mellin transforms, we have compared the new jointly resummed predictions to those obtained previously at fixed order as well as with pure p_T and threshold resummation. We found in general good agreement in the transverse momentum and invariant mass distributions, confirming the reliability of the joint resummation method. In most cases the new results were also even more precise, so that they can be considered the most reliable predictions for direct gaugino production available for the Tevatron and the LHC. They are therefore of great importance for supersymmetry searches and parameter determinations at these hadron colliders and should be taken as the basis for future experimental analyses.

Acknowledgments

We thank E. Conte and Y. Patois for their help with using the grid. This work has been supported by a Ph.D. fellowship of the French ministry for education and research and by

the Theory-LHC-France initiative of the CNRS/IN2P3.

- [1] H. P. Nilles, Phys. Rept. **110** (1984) 1; H. E. Haber and G. L. Kane, Phys. Rept. **117** (1985) 75; J. F. Gunion and H. E. Haber, Nucl. Phys. B **272** (1986) 1 [Erratum-ibid. B **402** (1993) 567].
- [2] T. Aaltonen *et al.* [CDF Collaboration], Phys. Rev. Lett. **101** (2008) 251801; R. Forrest [CDF Collaboration], arXiv:0910.1931 [hep-ex]; V. M. Abazov *et al.* [D0 Collaboration], Phys. Lett. B **680** (2009) 34.
- [3] G. Aad *et al.* [ATLAS Collaboration], arXiv:0901.0512.
- [4] G. Bayatian *et al.* [CMS Collaboration], J. Phys. G **34** (2007) 995.
- [5] V. Barger, R. Robinett, W. Keung and R. Phillips, Phys. Lett. B **131** (1983) 372; S. Dawson, E. Eichten and C. Quigg, Phys. Rev. D **31** (1985) 1581; D. A. Dicus, S. Nandi and J. Woodside, Phys. Rev. D **41** (1990) 2347; M. Klasen and G. Pignol, Phys. Rev. D **75** (2007) 115003.
- [6] G. Bozzi, B. Fuks and M. Klasen, Phys. Rev. D **72** (2005) 035016; D. Berdine and D. Rainwater, Phys. Rev. D **72** (2005) 075003; S. Bornhauser, M. Drees, H. K. Dreiner and J. S. Kim, Phys. Rev. D **76** (2007) 095020.
- [7] T. Gehrmann, D. Maitre and D. Wyler, Nucl. Phys. B **703** (2004) 147; G. Bozzi, B. Fuks and M. Klasen, Phys. Lett. B **609** (2005) 339; J. Debove, B. Fuks and M. Klasen, Phys. Rev. D **78** (2008) 074020; M. Klasen, arXiv:1005.3503.
- [8] G. Bozzi, B. Fuks, B. Herrmann and M. Klasen, Nucl. Phys. B **787** (2007) 1; F. del Aguila *et al.*, Eur. Phys. J. C **57** (2008) 183; B. Fuks, B. Herrmann and M. Klasen, Nucl. Phys. B **810** (2009) 266.
- [9] A. T. Alan, K. Cankocak and D. A. Demir, Phys. Rev. D **75** (2007) 095002 [Erratum-ibid. D **76** (2007) 119903].
- [10] W. Beenakker, R. Höpker, M. Spira and P. M. Zerwas, Nucl. Phys. B **492** (1997) 51; W. Beenakker, M. Krämer, T. Plehn, M. Spira and P. M. Zerwas, Nucl. Phys. B **515** (1998) 3; H. Baer, B. W. Harris and M. H. Reno, Phys. Rev. D **57** (1998) 5871; E. L. Berger, M. Klasen and T. M. P. Tait, Phys. Rev. D **59** (1999) 074024; W. Beenakker, M. Klasen, M. Krämer, T. Plehn, M. Spira and P. M. Zerwas, Phys. Rev. Lett. **83** (1999) 3780 [Erratum-ibid. **100** (2008) 029901]; E. L. Berger, M. Klasen and T. M. P. Tait, Phys. Lett. B **459** (1999) 165;

- E. L. Berger, M. Klasen and T. M. P. Tait, Phys. Rev. D **62** (2000) 095014 [Erratum-ibid. **67** (2003) 099901]; M. Spira, arXiv:hep-ph/0211145; L. G. Jin, C. S. Li and J. J. Liu, Eur. Phys. J. C **30** (2003) 77; L. G. Jin, C. S. Li and J. J. Liu, Phys. Lett. B **561** (2003) 135.
- [11] W. Hollik, M. Kollar and M. K. Trenkel, JHEP **0802** (2008) 018; W. Hollik, E. Mirabella and M. K. Trenkel, JHEP **0902** (2009) 002; E. Mirabella, JHEP **0912** (2009) 012.
- [12] G. Bozzi, B. Fuks and M. Klasen, Phys. Rev. D **74** (2006) 015001; M. Klasen, Nucl. Phys. Proc. Suppl. **160** (2006) 111; L. L. Yang, C. S. Li, J. J. Liu and Q. Li, Phys. Rev. D **72** (2005) 074026; H. K. Dreiner, S. Grab, M. Krämer and M. K. Trenkel, Phys. Rev. D **75** (2007) 035003; Y. Q. Chen, T. Han and Z. G. Si, JHEP **0705** (2007) 068.
- [13] J. Debove, B. Fuks and M. Klasen, Phys. Lett. B **688** (2010) 208; J. Debove, proceedings of the 2009 Europhysics Conference on *High Energy Physics* (EPS HEP 2009), Cracow, Poland, arXiv:0908.4149 [hep-ph].
- [14] G. Bozzi, B. Fuks and M. Klasen, Nucl. Phys. B **777** (2007) 157; C. S. Li, Z. Li, R. J. Oakes and L. L. Yang, Phys. Rev. D **77** (2008) 034010; A. Kulesza and L. Motyka, Phys. Rev. Lett. **102** (2009) 111802; U. Langenfeld and S. O. Moch, Phys. Lett. B **675** (2009) 210; A. Kulesza and L. Motyka, Phys. Rev. D **80** (2009) 095004; W. Beenakker, S. Brensing, M. Krämer, A. Kulesza, E. Laenen and I. Niessen, JHEP **0912** (2009) 041; W. Beenakker, S. Brensing, M. Krämer, A. Kulesza, E. Laenen and I. Niessen, JHEP **1008** (2010) 098.
- [15] J. Debove, B. Fuks and M. Klasen, Nucl. Phys. B **842** (2011) 51; J. Debove, proceedings of the 2010 Rencontres de Moriond on *QCD and High-Energy Interactions* (Moriond QCD 2010), La Thuile, Italy, arXiv:1009.2436 [hep-ph].
- [16] H. n. Li, Phys. Lett. B **454** (1999) 328.
- [17] E. Laenen, G. F. Sterman and W. Vogelsang, Phys. Rev. Lett. **84** (2000) 4296.
- [18] E. Laenen, G. F. Sterman and W. Vogelsang, Phys. Rev. D **63** (2001) 114018; A. Kulesza, G. F. Sterman and W. Vogelsang, Phys. Rev. D **66** (2002) 014011; A. Kulesza, G. F. Sterman and W. Vogelsang, Phys. Rev. D **69** (2004) 014012; A. Banfi and E. Laenen, Phys. Rev. D **71** (2005) 034003; G. Bozzi, B. Fuks and M. Klasen, Nucl. Phys. B **794** (2008) 46; B. Fuks, M. Klasen, F. Ledroit, Q. Li and J. Morel, Nucl. Phys. B **797** (2008) 322.
- [19] G. Altarelli and G. Parisi, Nucl. Phys. B **126** (1977) 298.
- [20] W. Furmanski and R. Petronzio, Z. Phys. C **11** (1982) 293.
- [21] S. Catani and L. Trentadue, Nucl. Phys. B **327** (1989) 323; S. Catani and L. Trentadue, Nucl.

- Phys. B **353** (1991) 183.
- [22] H. Contopanagos and G. Sterman, Nucl. Phys. B **419** (1994) 77.
- [23] S. Catani, M. L. Mangano, P. Nason and L. Trentadue, Nucl. Phys. B **478** (1996) 273.
- [24] C. Amsler *et al.* [Particle Data Group], Phys. Lett. B **667** (2008) 1.
- [25] Tevatron Electroweak Working Group, arXiv:0903.2503 [hep-ex].
- [26] P. M. Nadolsky *et al.*, Phys. Rev. D **78** (2008) 013004.
- [27] W. Porod, Comput. Phys. Commun. **153** (2003) 275.
- [28] V. Khachatryan *et al.* [CMS Collaboration], arXiv:1101.1628 [hep-ex].
- [29] M. Mühlleitner, A. Djouadi and Y. Mambrini, Comput. Phys. Commun. **168**, 46 (2005).
- [30] J. A. Aguilar-Saavedra *et al.*, Eur. Phys. J. C **46** (2006) 43.
- [31] B. C. Allanach *et al.*, in *Proc. of the APS/DPF/DPB Summer Study on the Future of Particle Physics (Snowmass 2001)* ed. N. Graf, Eur. Phys. J. C **25** (2002) 113.
- [32] M. Battaglia, A. De Roeck, J. R. Ellis, F. Gianotti, K. A. Olive and L. Pape, Eur. Phys. J. C **33** (2004) 273.